Supporting Information

Solvent-free fabrication of Ni$_2$P/UiO-66 catalyst for the hydrogenation of furfural to

cyclopentanone

Fanglin Liu, Luyao Li, Hui Hu, Mengting Yu, Dan Zhao, Shengjun Deng, Shunmin

Ding, Weiming Xiao*, Shuhua Wang, Chao Chen

Key Laboratory of Jiangxi Province for Environment and Energy Catalysis, School

of Chemistry and Chemical Engineering, Nanchang University, Nanchang, 330031, P.

R. China

E-mail: xiaoweiming@ncu.edu.cn.

Contents

Section S1 Experimental details

Materials

Zirconium tetrachloride (ZrCl$_4$) and furfural (FA) were purchased from Aladdin Biochemical Technology Co., Ltd.; N, N-dimethylformamide (DMF), methanol (CH$_3$OH), n-dodecane (C$_{12}$H$_{26}$), acetic acid (CH$_3$COOH), nickel nitrate hexahydrate (Ni(NO$_3$)$_2$·6H$_2$O) were obtained from Sinopharm Chemical Reagent Co., Ltd.; terephthalic acid (PTA) was acquired from Shanghai Wokai Pharmaceutical Co., Ltd.; sodium hypophosphite (NaH$_2$PO$_2$) was provided by Innochem Reagent Co., Ltd; H$_2$ was supplied by Jiangzhu Co., Ltd. All chemical reagents were used directly without further purification.

Synthesis of UiO-66

UiO-66 samples were prepared following a recipe reported by Behrens's group (a modulator approach).[1] UiO-66 samples were synthesized by solvothermal method. Zirconium tetrachloride and terephthalic acid were dissolved in DMF in equal molar ratio, and then acetic acid was added and stirred for 20 min. The mixture was then transferred into a polytetrafluoroethylene-lining autoclave and heated at 120 °C for 24 h. After the reaction, the product was collected by centrifugation, washing with DMF to remove the unreacted precursor, exchanging with methanol for three times and drying at 80 °C for 12 h.

Synthesis of 10%Ni$_2$P/UiO-66-I

Ni(NO$_3$)$_2$·6H$_2$O (99 mg) and UiO-66 (200 mg) were dispersed into 10 mL of water respectively, then the nickel nitrate aqueous solution was slowly dripped into UiO-66. Finally, the mixed solution was heated and stirred in an oil bath at 120 °C for 24 h until the water was evaporated to dryness to obtain the sample Ni(NO$_3$)$_2$/UiO-66. Subsequently, in N$_2$ atmosphere, Ni(NO$_3$)$_2$/UiO-66 and NaH$_2$PO$_2$ were placed at two separate positions in a quartz tube, and NaH$_2$PO$_2$ was placed at the upstream side of the quartz tube. The mass ratio of Ni(NO$_3$)$_2$/UiO-66 to NaH$_2$PO$_2$ is 2:1 and the two are separated by quartz cotton. Then the quartz tube was heated to 300 °C with a ramp rate

of 2 °C / min and then maintained at this temperature for 2 h. After naturally cooling to room temperature, the 10%Ni$_2$P/UiO-66-I was obtained.

Section S2 Characterization

Powder X-ray diffraction

The powder X-ray diffraction (XRD) patterns of the samples were performed on a Rigaku SmartLab 9kW X-ray diffractometer with Cu Kα (λ = 1.542 Å) as the radiation source. The sample was scanned at a rate of 50 °/min, and the angle (2θ) ranged from 4° to 80°.

ICP-OES

Agilent Technologies 5100 inductively coupled plasma optical emission spectrometer (ICP-OES) was used to analyze the aqua regia of each part of the completely dissolved catalyst, and the actual components of Ni and P in the catalyst samples were determined.

N$_2$ adsorption/desorption isotherms at 77 K

N$_2$ adsorption-desorption isotherms were analyzed on an Autosorb-iQ analyzer (Quantachrome) at 77 K. Prior to analysis, about 50 mg of the fresh catalyst was activated at 150 °C under high vacuum for 12 h. The surface areas were calculated by the multi-point BET (Brunauer–Emmett–Teller) method, and micropore surface areas were estimated by t-plot equation. Pore size distributions were derived from the nonlocal density functional theory model.

X-ray photoelectron spectroscopy

X-ray photoelectron spectroscopy (XPS) measurements were performed on a Thermo Scientific K-Alpha X-ray spectrometer. The binding energy was corrected by the C 1s peak (284.8 eV) of the amorphous carbon.

H$_2$ temperature programmed desorption (H$_2$-TPD)

H$_2$-TPD was carried out on a Micromeritic-Auto-Chem II 2920 chemisorption analyzer combined with a thermal conductivity detector and a computer-controlled furnace.

Before measurement, about 50 mg of the fresh catalyst was placed in a U-shaped quartz tube and pretreated at 200 °C in pure argon (30 mL/min) for 60 min in order to eliminate air components that might be adsorbed on the fresh sample during the transfer process. For H_2-TPD measurements, the system was cooled to room temperature under the protection of argon and saturated by flowing H_2 (30 mL/min) for 30 min, then pure argon was switched into the system again to purge free adsorbed H_2 for 30 min, subsequently, the sample was heated to 300 °C at a heating rate of 10 °C/min and desorption signals were simultaneously reflected by TCD detector.

Catalytic hydrogenation of FA

The catalytic hydrogenation rearrangement of FA to CPO were all performed at 150 °C under 0.5 MPa H_2 in a 50 mL Teflon reactor with a stainless-steel autoclave heater equipped with liquid-sampling device. Typically, the reaction mixture was composed of 1 mmol FA, 50 mg catalyst and 15 mL water; prior to the reaction, the reaction system was purged 6–8 times with H_2 to exclude air, and then the system saturated by 0.5 MPa H_2 was closed with the program was set to heat the autoclave from 25 to 150 °C at a speed of 10 °C/min under magnetic stirring for 10 h at 400 rpm. Once the reaction kettle was cooled to room temperature, the liquid products were separated by extraction with ethyl acetate. For catalytic cycle test, the used catalyst was separated out of solution by centrifugation and dried in vacuum, then added in fresh reaction solution to perform next cycle test following above procedure. The composition of reaction solution was analyzed by gas chromatograph-mass spectrometry on an Agilent 7890B-5977A apparatus, equipping an Agilent 19091S-433 capillary column (HP-5MS, 30 m × 250 μm × 0.25 μm). According to the previously determined standard composition curves for both FA and CPO, the composition of reaction mixtures were calibrated simultaneously to calculate FA conversion and CPO yield, respectively, the analytical error is calibrated within 3%, based on the average results from three repeated measurements at least. The conversion, product selectivity, TON and carbon balance were calculated by the following:

$$\text{Conversion (\%)} = (1 - \frac{moles\ of\ residual\ furfural}{moles\ of\ initial\ furfural}) * 100\%$$

$$\text{Selectivity (\%)} = \frac{\textit{moles of target product}}{\textit{moles of total products}} * \textit{100\%}$$

$$\text{TON} = \frac{\textit{moles of reacted Furfural}}{\textit{moles of Ni}_2\textit{P on the catalyst}}$$

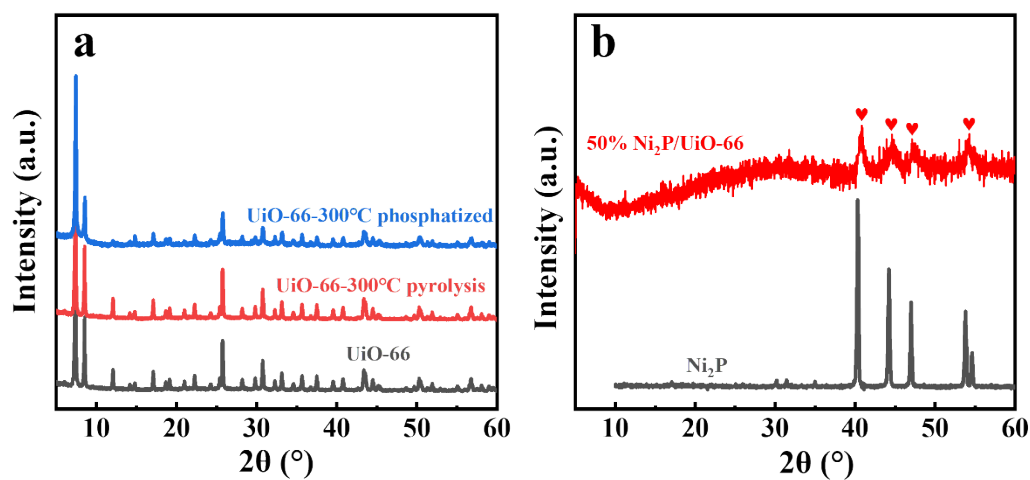$$\text{Carbon balance (\%)} = \frac{\textit{moles of total products}}{\textit{moles of reacted Furfural}} * \textit{100\%}$$

Section S3 Figures

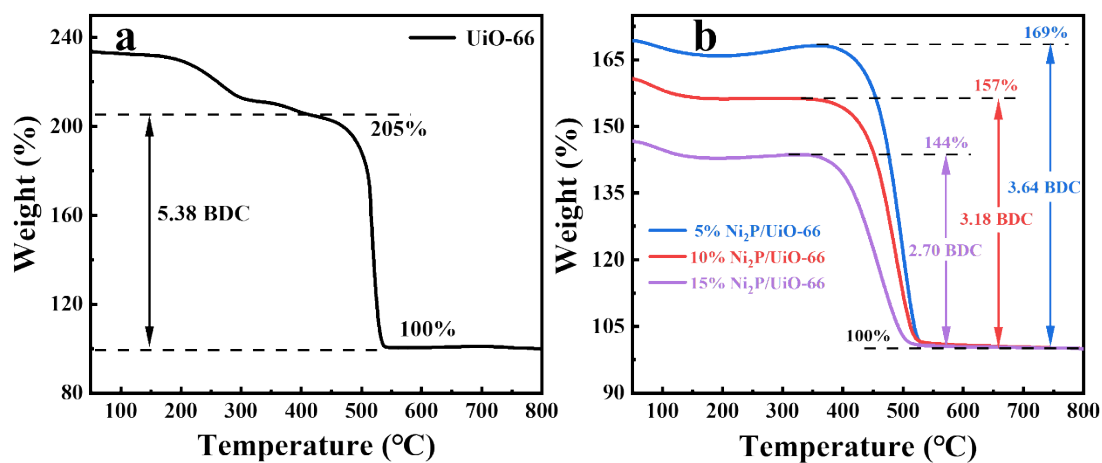**Figure S1.** XRD patterns of UiO-66, UiO-66-300 °C pyrolysis and UiO-66-300 °C phosphatized (a); 50%Ni_2P/UiO-66 and simulated Ni_2P (b).

Figure S2. TGA curves of UiO-66 (a); 5%Ni_2P/UiO-66, 10%Ni_2P/UiO-66 and 15%Ni_2P/UiO-66 (b).
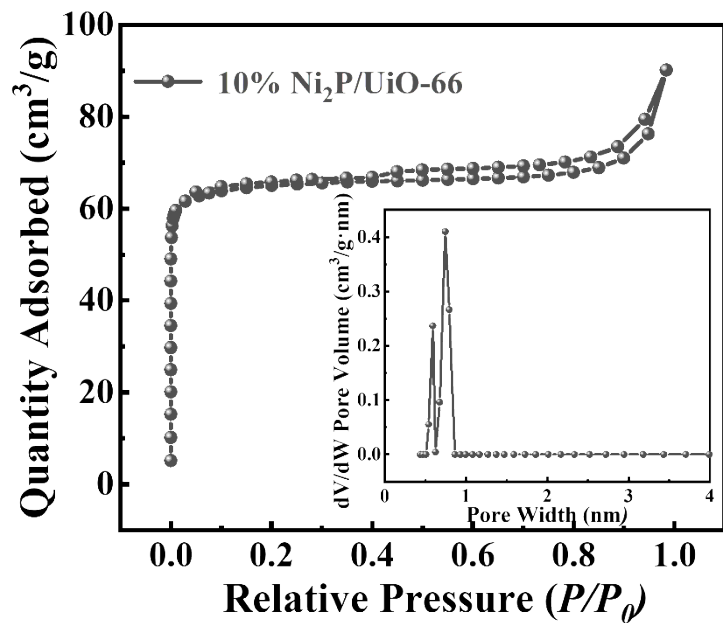
Figure S3. Ar adsorption-desorption isotherm and pore size distribution of 10%Ni$_2$P/UiO-66.
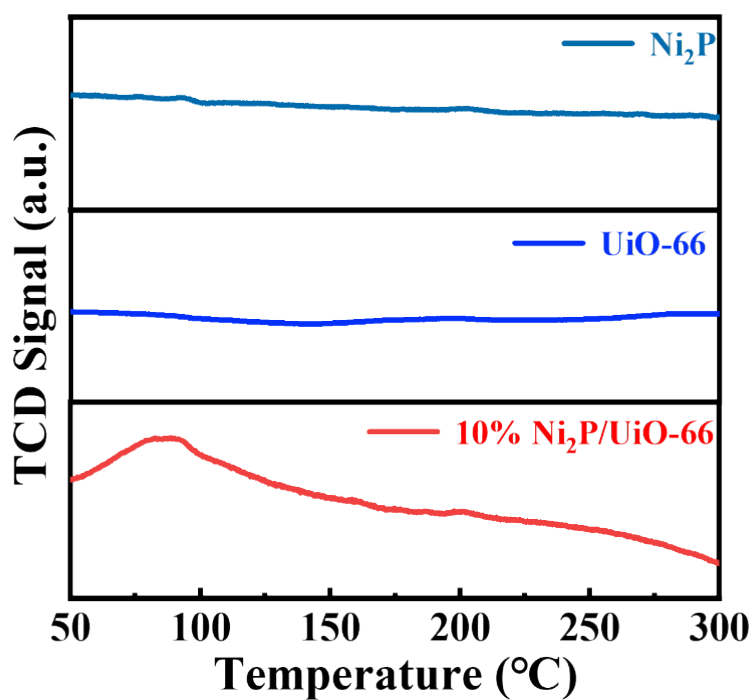
Figure S4. H$_2$-TPD profiles of Ni$_2$P, UiO-66 and 10%Ni$_2$P/UiO-66.
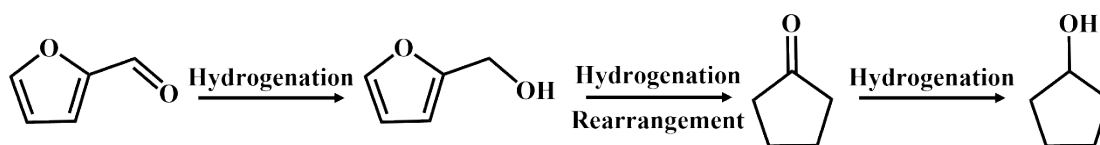
Figure S5. The profile of furfural conversion.
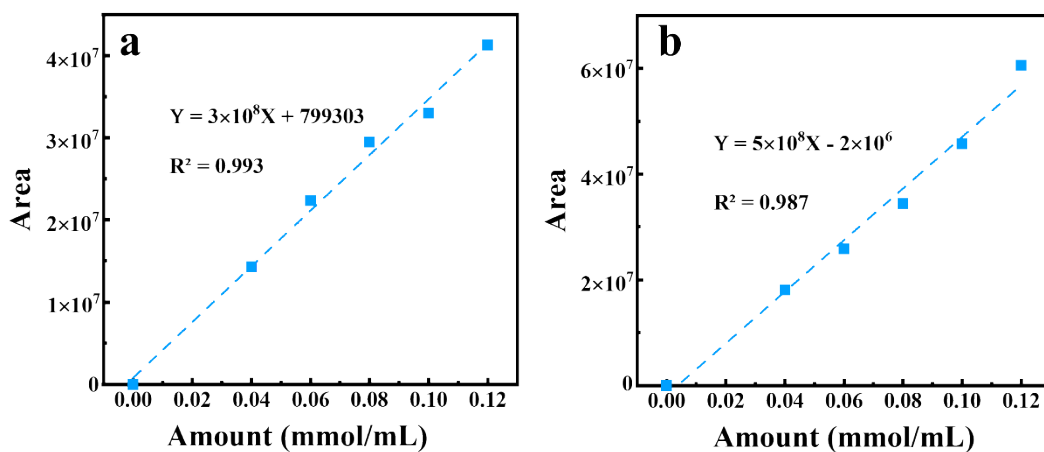
Figure S6. The standard curves of (a) FA and (b) CPO.
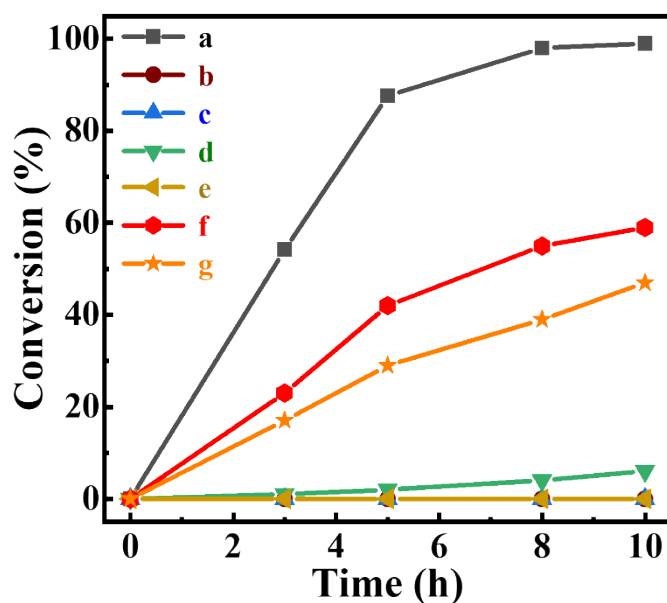
Figure S7. Comparative experiments of FA hydrogenation catalyzed by different catalysts (a) 10%Ni$_2$P/UiO-66, (b) UiO-66, (c) UiO-66 pyrolysis, (d) Ni$_2$P, (e) UiO-66 phosphatized, (f) 10%Ni$_2$P/TiO$_2$, and (g) 10%Ni$_2$P/Al$_2$O$_3$.
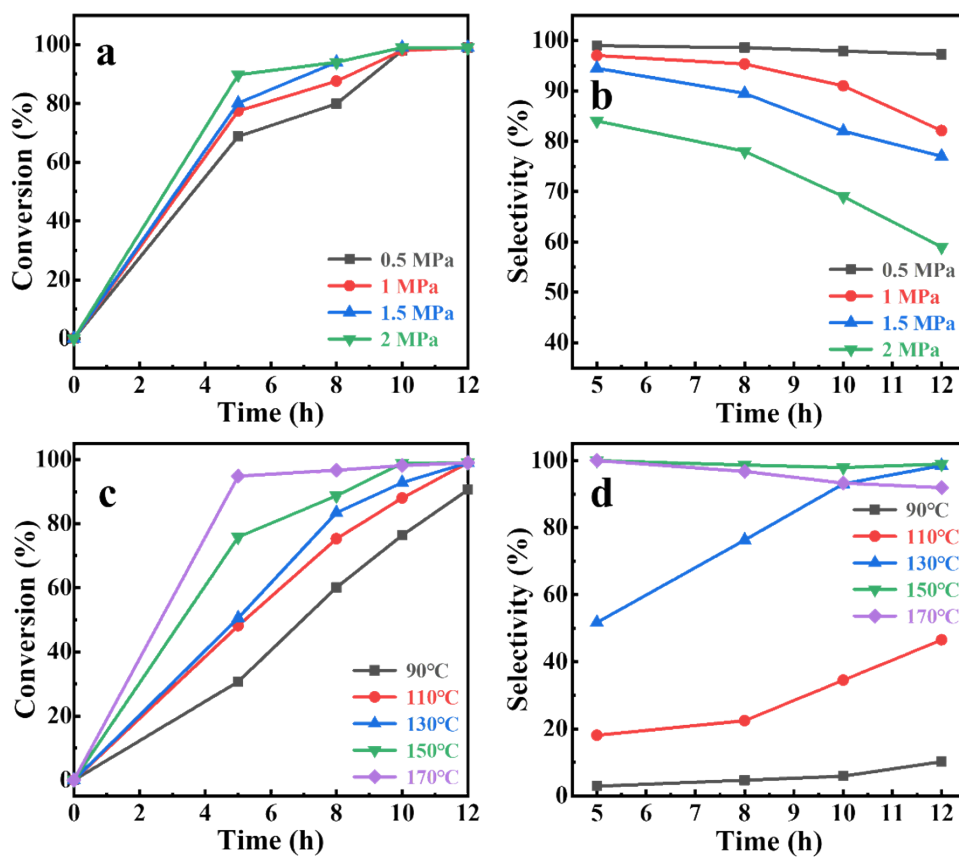
Figure S8. Optimized the reaction conditions over 10%Ni$_2$P/UiO-66 catalyst: (a) and (b) H$_2$ pressure; (c) and (d) reaction temperature.
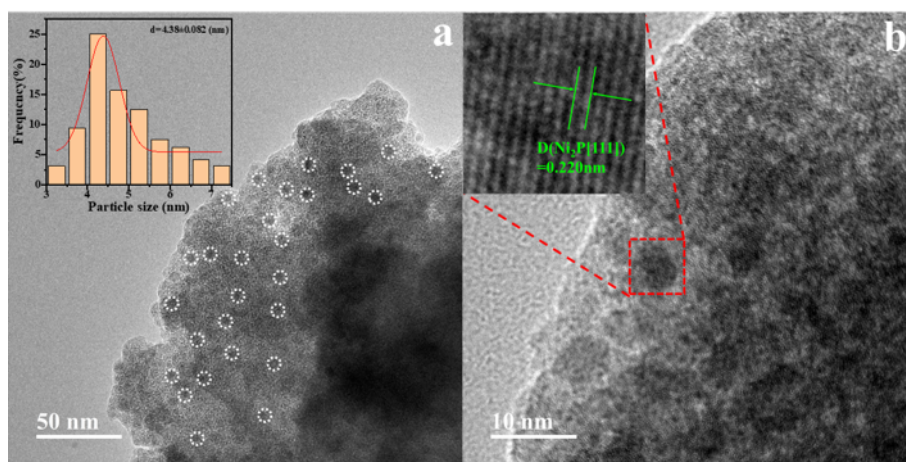
Figure S9. Bright-field TEM images and particle size distribution of 10%Ni$_2$P/UiO-66-I.
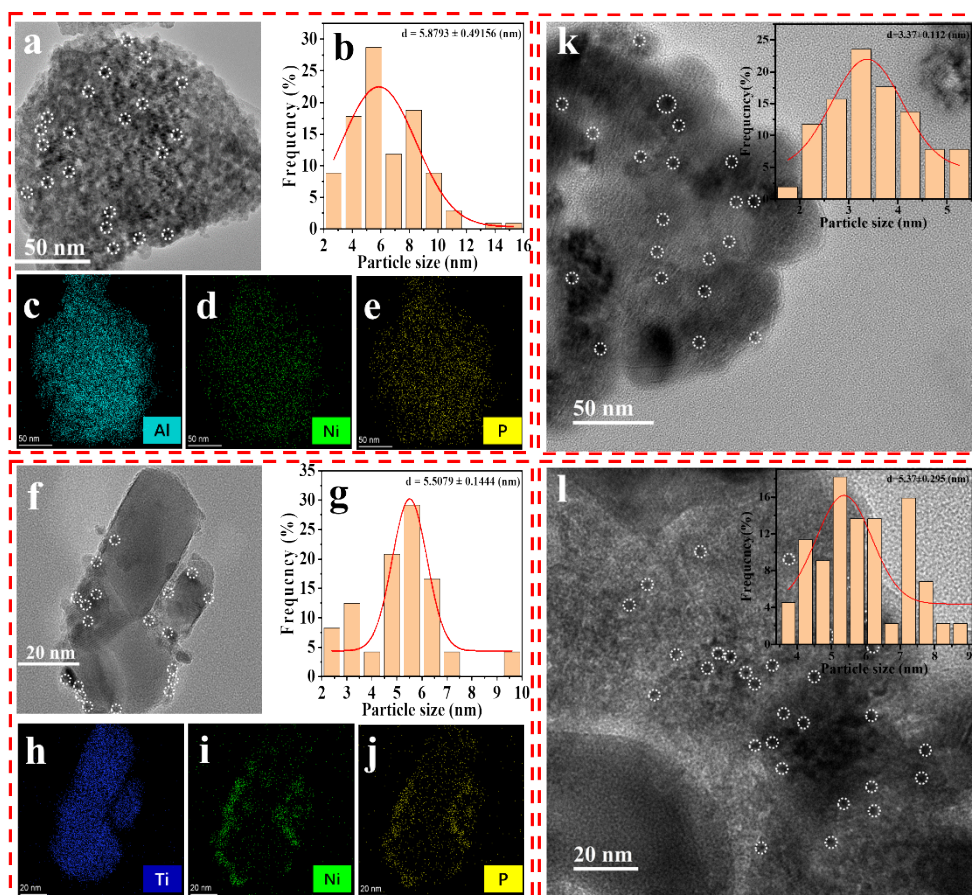
Figure S10. Bright-field TEM images, EDS mappings and particle size distributions of (a-e) 10%Ni$_2$P/Al$_2$O$_3$, (f-j) 10%Ni$_2$P/TiO$_2$, (k) 10%Ni$_2$P/SiO$_2$ and (l) 10%Ni$_2$P/ZrO$_2$.
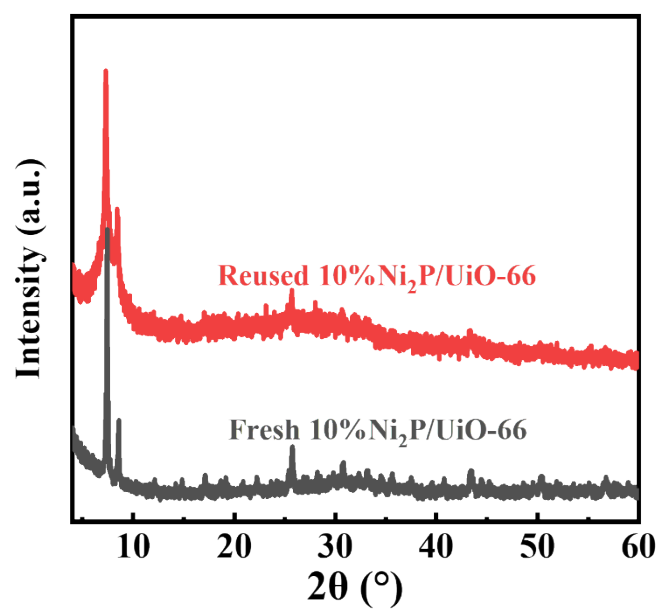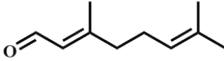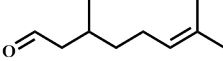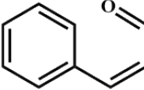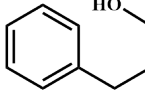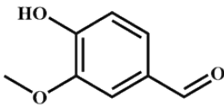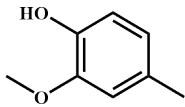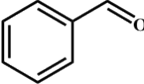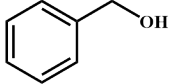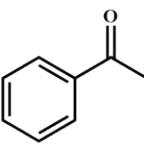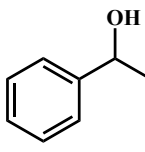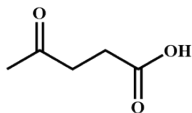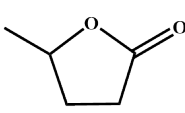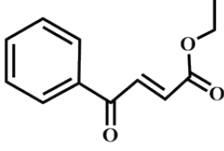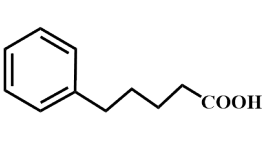

Figure S11. XRD patterns of 10% Ni$_2$P/UiO-66 before and after five recycles.

Section S4 Table

Table S1 Results of catalytic hydrogenation of aldehydes/ketones.

Entry	Reaction substrate	Product	Yield (%)	Temp . (K)	P_{H_2} (MPa)	Time (h)
1			97.3	373	2	3h
2			90.5	433	1.5	8h
3			99	423	1	8h
4			91.7	353	0.5	10h
5			99	353	0.5	10h
6			90	373	1	10h
7			99	423	2	10h

Reaction conditions: substrate (1 mmol), isopropanol (15 mL), catalyst (50 mg), speed (400 rpm).

For the hydrodeoxygenation product of entry 3, in fact, many works have demonstrated that the hydrodeoxygenation product are often observed in the hydrogenation of Vanillin. And the Ni_2P-based catalysts have been proved to exhibit superior hydrodeoxygenation performance. The excellent hydrodeoxygenation ability

11

of Ni_2P could be attributed to the high d-electron density of Ni sites that favors the aldehyde group adsorption and C–O bond cleavage[2-3].
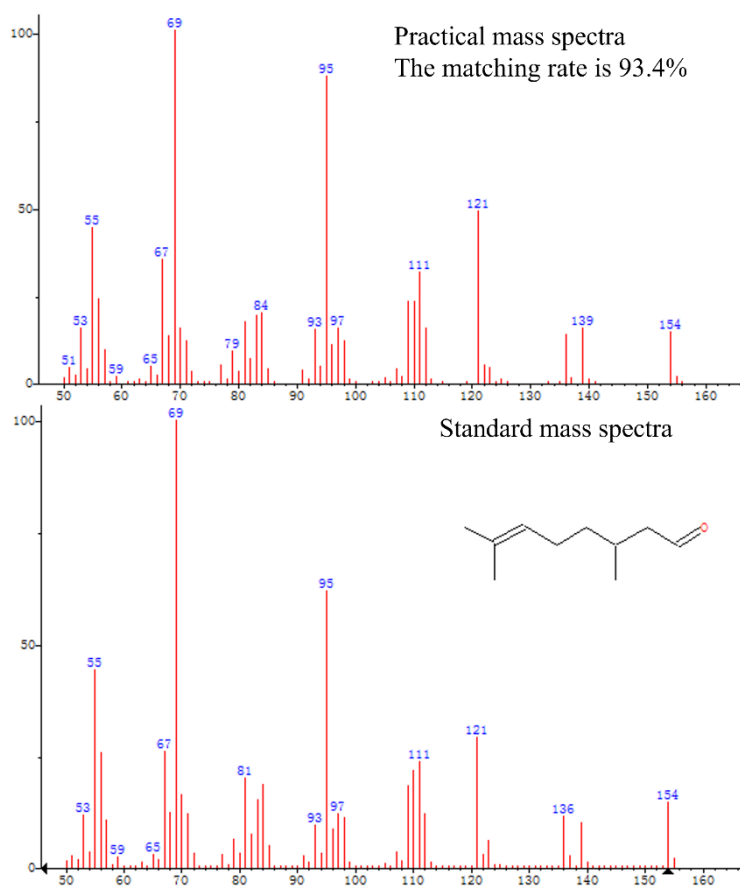
Section S5 Figures

Figure S12. The practical and standard mass spectra of citronellal.
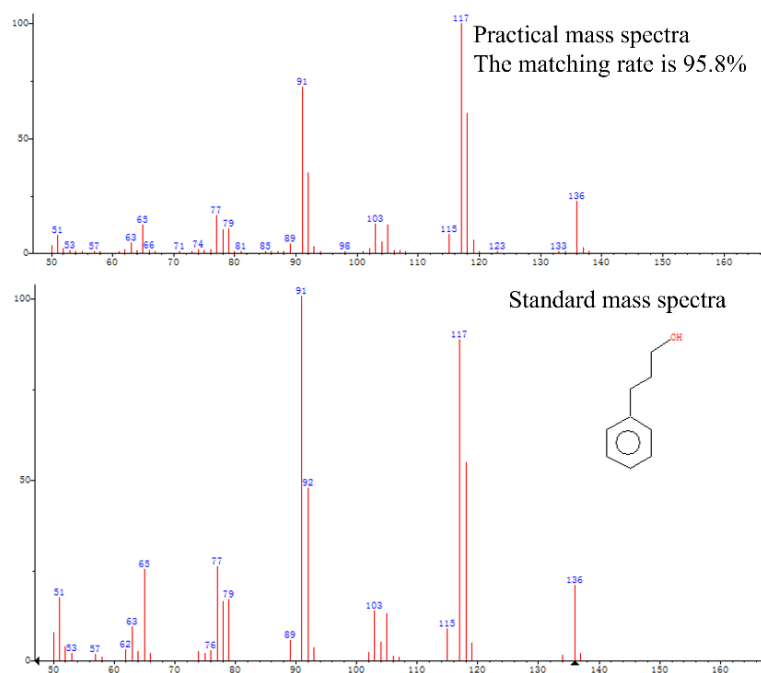
Figure S13. The practical and standard mass spectra of 3-Phenylpropanol.
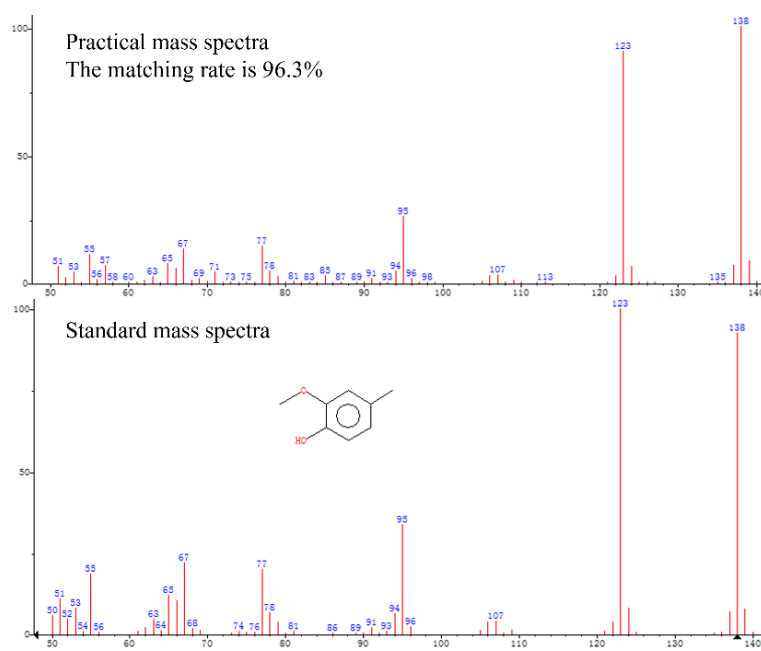

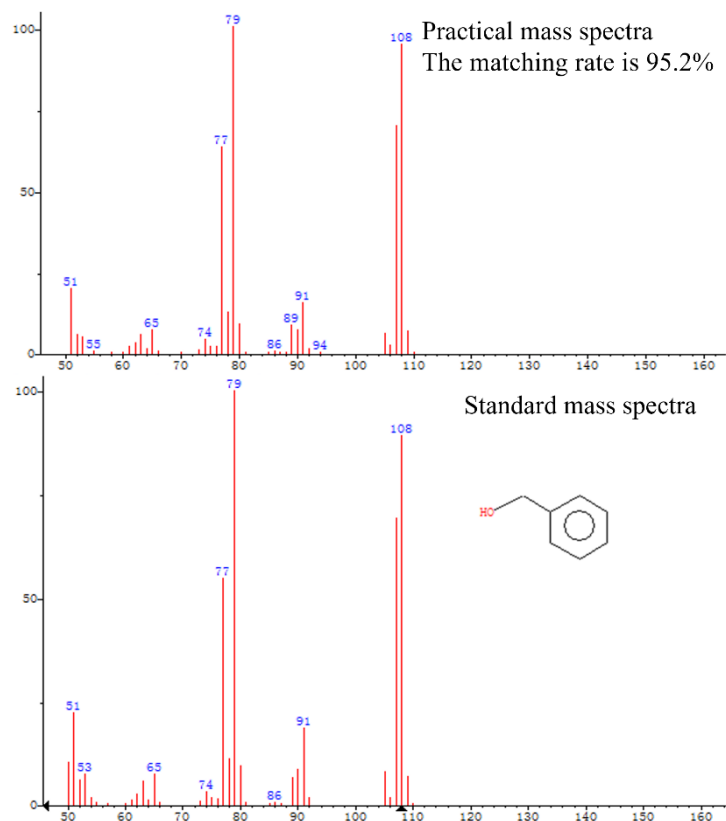**Figure S14.** The practical and standard mass spectra of creosol.

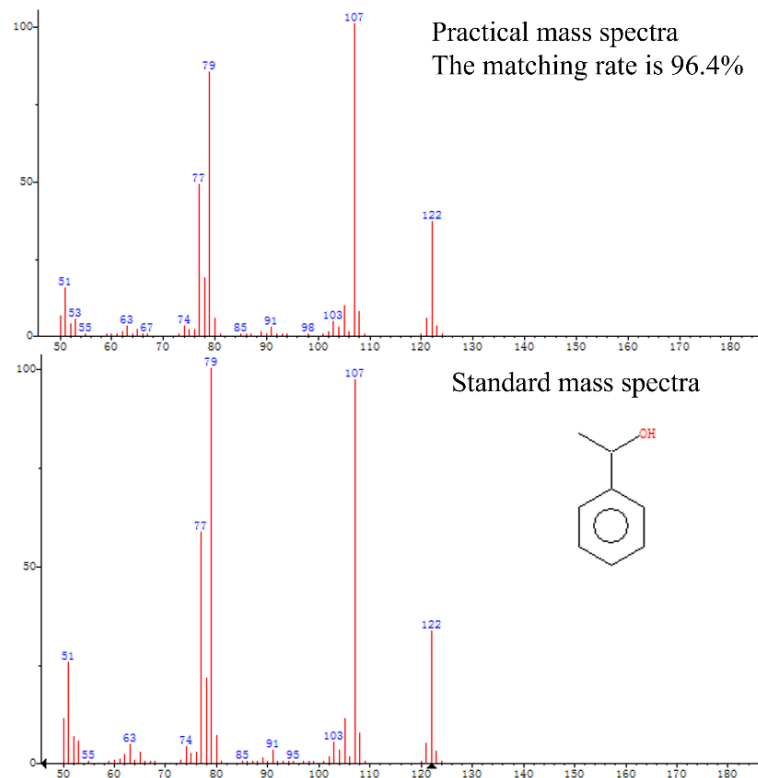**Figure S15.** The practical and standard mass spectra of benzyl alcohol.

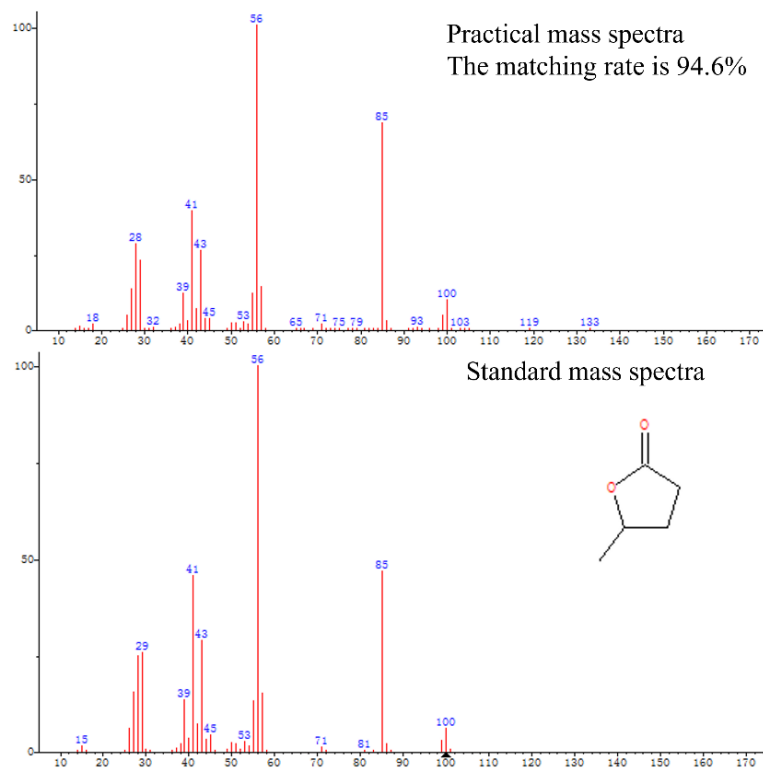**Figure S16.** The practical and standard mass spectra of α-Phenethyl alcohol.

Figure S17. The practical and standard mass spectra of gamma-valerolactone.
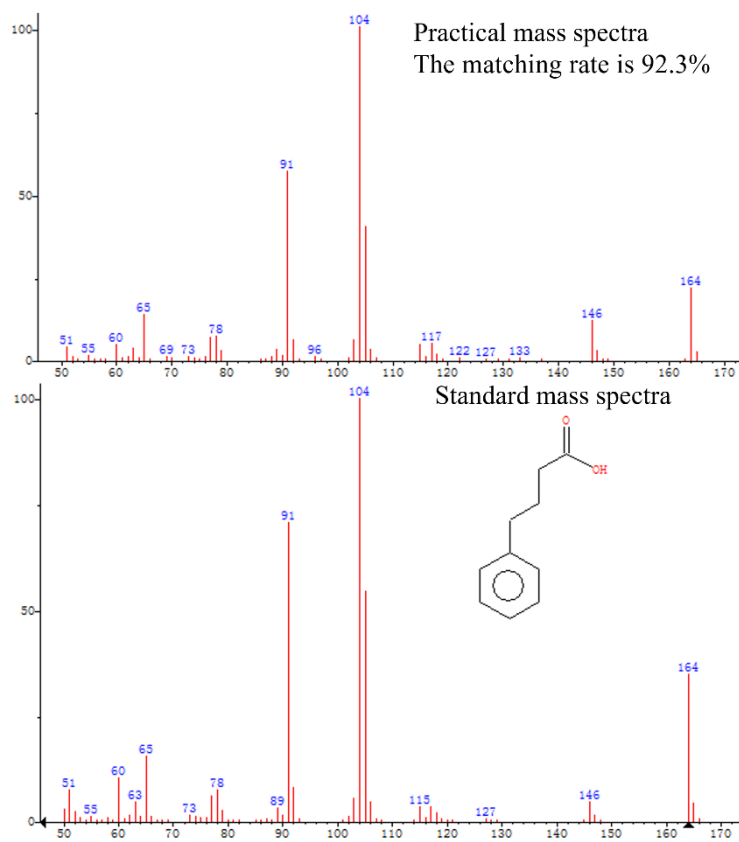

Figure S18. The practical and standard mass spectra of benzenebutanoic acid.

Reference

1. A. Schaate, P. Roy, A. Godt, J. Lippke, F. Waltz, M. Wiebcke and P. Behrens, *Chem. Eur. J.*, 2011, **17**, 6643-6651.
2. V. O. O. Gonçalves, P. M. de Souza, T. Cabioc'h, V. T. da Silva, F. B. Noronha and F. Richard, *Appl. Catal. B,* 2017, **219**, 619-628.
3. A. Berenguer, J. A. Bennett, J. Hunns, I. Moreno, J. M. Coronado, A. F. Lee, P. Pizarro, K. Wilson and D. P. Serrano, *Catal. Today,* 2018, **304**, 72-79.